Challenge Journal of Structural Mechanics

Review

A discussion on the beam on elastic foundation theory

Tunay Uzbay Yelce [a], Erdem Balcı [a,*], Niyazi Özgür Bezgin [a]

[a] *Department of Civil Engineering, İstanbul University-Cerrahpaşa, 34320 İstanbul, Türkiye*

ABSTRACT

A railway track is a structural composure of many elements. Railway track analyses requires analyses for the interaction between these elements and the interaction between the track and the vehicle passing over the track. Various design models have been developed to simplify the analysis of railway tracks and to establish appropriate design criteria. Winkler's representation of the subgrade support as a continuous structure with independent springs was adapted to railway tracks by Zimmermann that further evolved into what is known as the Beam on Elastic Foundation Theorem (BOEF) today. A soil and structure interaction model based on BOEF theorem, frequently used by engineers to analyze the response of continuously supported structures on bearing layers, provides estimates for the distribution of deflections, bearing pressure, shears and moments along a continuously supported structure, such as a plate, by subgrade. This study aims to provide an in-depth and an explicit solution to the 4th order differential equation of BOEF and serve as a resource for those who are interested in this topic. This study will also present the historical development of the BOEF model, its use in railway track analysis, as well as its underlying assumptions in terms of structural behavior.

ARTICLE INFO

Article history:
Received 12 June 2022
Revised 1 October 2022
Accepted 31 October 2022

Keywords:
Beam on elastic foundation
Winkler
Talbot
Zimmermann
Railway track analysis

1. Introduction

Transportation engineering is a field of civil engineering dedicated to developing means and methods to ensure the presence of a number of people or a quantity of goods (number, quantity), at a certain location (distance), reliably at a given condition (comfort, serviceability, safety), within a certain period of time (time). Railway transportation is a significant symbol of industrial revolution and mechanization of humanity that allowed humanity to transport, greater number of people and greater amount of goods, to further distance within smaller time intervals, reliably, comfortably and safely. To ensure this advancement, early engineers designed heavier vehicles known as trains along specially designed routes known as railway tracks. The intense forces exerted on railway tracks by the trains and the response of the track to these forces posed a significant challenge for the early engineers to qualitatively assess and quantify. Absence of the necessary geotechnical knowledge, mechanical theories, thermodynamic theories and metallurgical knowledge at the time, posed even a greater challenge since the necessary theoretical framework to respond to the necessary design challenges was absent. While the development of the railway tracks was mostly based on experimental –trial and error- based research in its early days, it evolved further with mathematical analysis after the second half of the 1800's (Kerr 2003). A ballasted railway track consists of steel rails, rail fasteners, timber, concrete, composite or steel sleepers, ballast layer, sub-ballast layer, which is also known as protective layer and subgrade materials. Occasionally, railway tracks can also include rail pads and under sleeper pads if required. The interaction between these elements due to their different mechanical properties makes the understanding of track structural behavior challenging. It is found to be practical to consider each track component as a single structural unit, so that one may observe the interaction between these units through the definition of suitable boundary conditions and load transfer patterns (Sadeghi and Barati 2010). However, not only the interaction between the in-

* *Corresponding author*. E-mail address: erdembalci@outlook.com (E. Balcı)
ISSN: 2149-8024 / DOI: https://doi.org/10.20528/cjsmec.2023.01.004

ternal elements of the track effects the reaction of the track to the wheel forces; but also the interaction between the track and the vehicle passing over the track and the interaction between the soil and structure, also effect the response of the track as well (Balcı et al. 2022). Therefore, the interaction between the rail elements as well as train-track interaction and soil-track interaction has to be examined to analyze railway tracks and determine design criteria.

Two types of track were to be analyzed; longitudinal-tie track and cross-tie track. In the first one, the track is assumed to be supported continuously, while, in the latter track is supported discretely by cross-ties that are also known as sleepers. Fig. 1 shows the comparison of the longitudinal-tie tracks with the cross-tie tracks. Even though, discussions are made on the "continuity" assumption of a discretely supported railway track, deep rail sections over ties with limited tie spacing enhanced the justification of the application of the analyses of a continuously supported track to discretely supported track over time. Detailed discussions and historic development of these two types of tracks can be found in the related work (Kerr 1976).

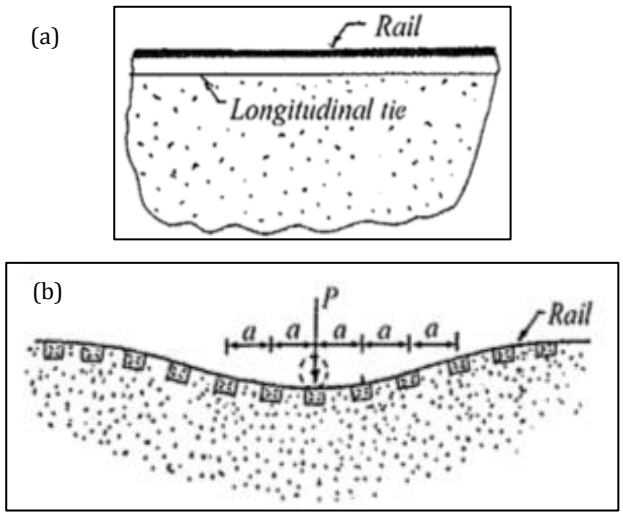

Fig. 1. Physical problem of: (a) Longitudinal-tie; (b) Cross-tie tracks (Kerr 2003).

Emil Winkler (1867) proposed a classical mathematical model to simplify the complex behavior of the soils by representing the soil with elastically deformable springs. Winkler's equation shed light on the analysis of railway tracks. Zimmermann's method idealized the railway track as a continuously supporting beam resting on a Winkler's foundation. However, in reality, the track is only supported at regular intervals (sleeper spacing), therefore, a discrete support model is developed. Heténi (1946) also developed some equations considering the boundary conditions in the railway track. These steps historically developed the beam on elastic foundation (BOEF) theory which is still in use to analyze railway tracks analytically. Finally, Talbot's experimental and analytical work showed the applicability of the BOEF theorem to the analyses of railway tracks (Kerr 2003).

This paper presents the development of the BOEF model to analyze longitudinal-tie and cross-tie tracks. The 4th order differential equation of the BOEF model is solved step by step so that one can obtain the necessary equations to determine deformation, moment, and shear forces. The shortcoming of the BOEF model is discussed. Finally, the continuous rail and discontinuous rail cases are compared according to the BOEF model.

2. Analysis of Railway Tracks

Railway tracks are complex structures to analyze due to fact that various components with different properties combine and interact with each other and they lay on a soil that is not fully homogenous. However, various researchers simplified the problem by making some assumptions and they developed mathematical models. The following explains the fundamental and practical models that are still in use and that led to the development of the BOEF theory.

2.1. Winkler model and subgrade modulus

Winkler developed a model to represent soil so that one can understand soil-track interaction better. Winkler Model describes the soil as linear, independent, elastic, closely located, and with an infinite number of springs. When a load is applied on a plate, the plate responds to this loading in relation to the mechanical qualities of the subgrade as well as the relative relation of the stiffness of the plate, which is the bending stiffness, with the compressive stiffness of the subgrade, which is a manifested quantity in relation to the bearing area of the plate and its bending stiffness. Fig. 2 is a general representation of a vertically loaded plate in three dimension, with a length L defined along the x-axis and width B defined along the y-axis with a bending rigidity of EI where E is the elastic modulus of the plate material and I is the moment of inertia of the plate along it's relevant bending axis. This plate is loaded by a generalized representation of distributed force defined as $f(x, y)$ which can be variable along the x and y axis. As a result of this applied force and in relation to the relative bending stiffness of this plate with respect to the compressive stiffness manifested in the subgrade, soil reaction denoted as $p(x, y)$ appears underneath the plate as a result of the soil deflection $w(x, y)$, which is not shown in this figure in order to maintain the clarity of the figure. Within the simplicity of the statement above, lies an important fundamental aspect of soil and structure interaction such that the soil reaction or in other words the substructure reaction is interrelated to the structural stiffness of the superstructure, which is the plate. The response of the supporting subgrade is not an independent and an isolated quality of the subgrade but a quality that varies with the stiffness of the supported structure. Emil Winkler, in his struggle to describe the generalized response of a structure supported by soil, represented the soil as a distribution of mechanically independent springs that elastically deform $w(x, y)$ under the pressure $f(x, y)$. Winkler's

model correlates the vertical contact pressure $p(x, y)$ at an arbitrary point in the underneath the plate to the corresponding vertical deformation $w(x, y)$ by using a coefficient, which is the "coefficient of vertical subgrade reaction" denoted by the term C in Eq. (1). Other symbols such as n_v and k_v, can also be used in liu of C, which is chosen to represent coefficient of vertical subgrade reaction in this study.

$$p(x, y) = C.w(x, y) \tag{1}$$

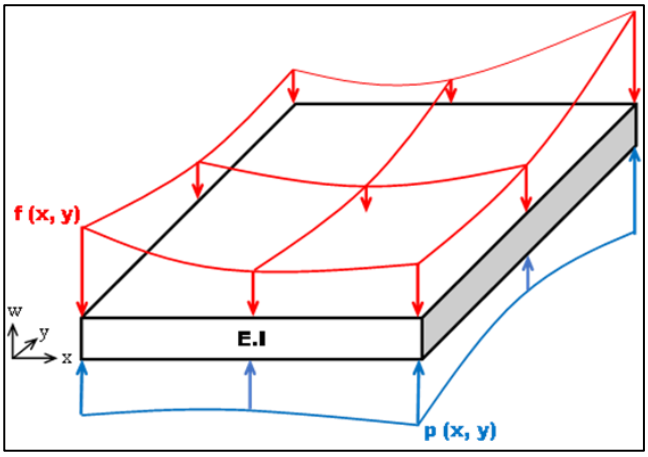

Fig. 2. Representation of a plate loaded by distributed load $f(x,y)$ and supported by the pressure generated by the subgrade $p(x,y)$.

The coefficient of vertical subgrade reaction is the ratio of the pressure at a particular point underneath a surface structure to the vertical deflection measured for that particular location (Terzaghi 1955). However, the coefficient of vertical subgrade reaction is not only affected by the subgrade material but also by the mechanical and geometrical properties of the superstructure. As its name implies, it is a particular reaction the subgrade gives to a loading by a particular structural element. In other words, the same subgrade would react differently to structures with different bending stiffness values and contact areas with the subgrade. Terzaghi (1955) investigated the change in stress distribution and the variation of the coefficient of vertical subgrade reaction with respect to the changes in superstructure qualities.

Winkler Model does not consider the vertical deformation in the soil springs located outside and underneath plate loading area due to shear transfer within the soil continuum (Skar et al. 2019). This leads to discontinuity of vertical deformation at the edges of the loaded area as shown in Fig. 3. Normally, the shear stresses would couple the deformation of adjacent springs and therefore there had to be a continuity in the deformation at the edges of the loading area (Worku 2009). However, shear stresses are not considered in the Winkler approach and thus, a spring undergoes the deformation independently of the neighboring springs (Horvath 1983a). Various attempts have been made to include the effect of shear stress. Some of them are Horvath (2002), Horvath (1983b), Kerr (1964), Reissner (1958), Worku (2009), and Onu (2000).

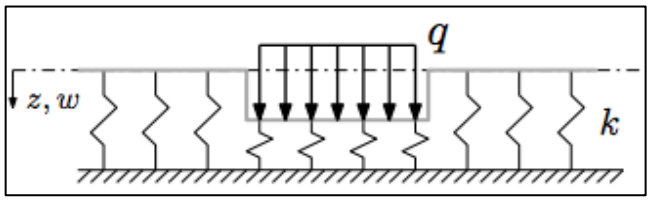

Fig. 3. Winkler soil model and the deformations (Skar et al. 2019).

Two-parameter model of Pasternak (1954) uses a second parameter k_2 to consider shear reactions of the foundation in addition to the first (Winkler) parameter k_1. Poddubny and Gordon (2021) concludes that shear rigidity vanishes when there is a sudden change in the physical and mechanical features of the foundation. Therefore negative effects caused by sudden changes in track should be considered in beams resting on elastic base models.

Two-parameter model of Vlasov and Leont'ev (1966) considers the depth of the soil layer under the foundation in addition to the shear forces and shear strain energy. While the foundation is modelled as an elastic layer, deflections within the foundation is restricted to an appropriate mode shape, $\varphi(z)$ by using constraints. However, a method for the determination of the parameter used for the decay of the stress distribution, γ is not proposed by the authors. Jones and Xenophontos (1977) correlated the γ and the displacement characteristics. Later, Vallabhan and Das (1988) determined γ as a function of the characteristics of the beam and the foundation.

Datta and Roy (2002), Wang et al. (2005), Balabušić et al. (2019), Tivari and Kuppa (2014), and Campione et al. (2021) evaluate and discuss the models established for the interaction between the structures and elastic foundations. Even though the assumptions it made, the Winkler Model is widely preferred among engineers due to its simplicity.

Application of the Winkler model, to railway tracks with discrete ties supports, has raised concern with regards to its applicability. However, Talbot's experimental work led by a team of railway experts, showed that the spacing between the discrete tie supports could be neglected and that the Winkler's continuously supported beam model can be applied to railway tracks as well (Kerr 2003). The depth of the rails in relation to the spacing of the ties is significant and therefore the rail acts as a deep-beam between the ties generating significant bending and shear stiffness thus providing continuity between the ties (Bezgin 2018).

Further studies are conducted to include different aspects of the elastic foundation-structure interaction. Abouelregal (2020) investigated the coupling between deformation and the temperature field caused by ultrafast laser heating for a beam resting on Winkler foundation. Froio et al. (2021) numerically modelled the moving load beam problem to effectively resolve the dynamic response of beams subjected to high velocity moving load. Thomas et al. (2020) investigated the applicability of almost incompressible elastomeric layers to the Winkler model by deriving a model that interpolates be-

tween the incompressible limits for thin elastic layers. Authors conclude that Poisson ratio and a compressibility parameter (related to layer's slenderness) are effective on the applicability of Winkler model. Aizikovich et al. (2016) examined the relationship between the interlayer thickness, gradient of elastic properties and the distribution of the contact stress under the beam.

2.2. Zimmermann model and track modulus

In the 1880s, Zimmermann applied the Winkler Model to the railway tracks by considering rails as constantly supported beams resting on the soil. Zimmermann adopted this approach in an attempt to fully comply the adoption of a continuously supported structure for a discretely supported railway track structure. While the supported part of the structure is the rails, the supporting parts are the sleepers/slab and the underlying layers. In the railway application, the rails are modeled as two parallel continuous beams constrained by the sleepers at regular intervals (sleeper spacing). Since the sleepers are supported by the underlying layers as well as the two sides of the sleeper, it is assumed that there is no deformation in the sleeper. The idea behind the Zimmermann method is to determine the supported area of a single beam and then transfer bearing areas into a continuously supported beam (Prakoso 2012).

In Fig. 4, l is the length of sleeper, m is the length of sleeper without support, b_1 is the width of sleeper, b is the width of the beam, and a is the sleeper spacing.

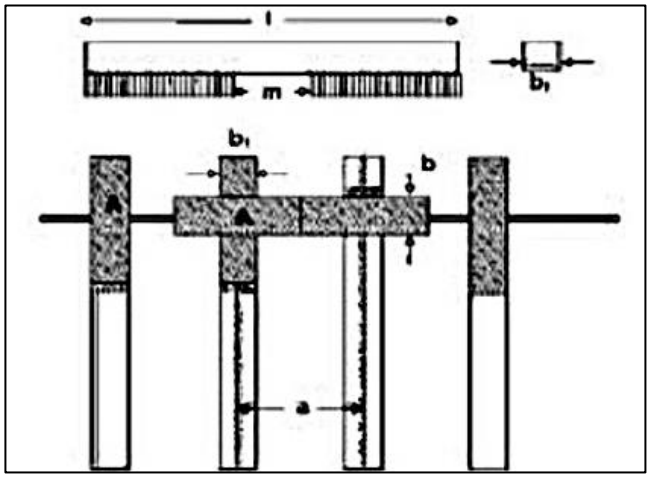

Fig. 4. Supporting areas in the Zimmermann model (Steidl 2007).

The supported area of one sleeper $F = (l - m) * b_1/2$ can be connected to the support areas of adjacent sleepers so that theoretical continuous rail support can be provided. The length of the transformed area is the sleeper spacing (a) and the width of it is the $b=F/a$. In order to include the response of the track, a single representative value is used in the model that has the same units of $Force/Length^3$ as in the coefficient of vertical subgrade reaction. However, in reality, the track consists of various elements with different responses. Therefore, a combined value representative value (C_{total}) of these elements must be used as shown in Eq. (2).

$$\frac{1}{C_{\text{total}}} = \frac{1}{C_{\text{railpad}}} + \frac{1}{C_{\text{ballast}}} + \frac{1}{C_{\text{subballast}}} + \frac{1}{C_{\text{subsoil}}} \tag{2}$$

The characteristic length of the structure can be determined through Eq. (3).

$$L = \sqrt{\frac{4.E.I}{b.C}} \tag{3}$$

The deflections and bending moments at a specific location can be calculated by using an influence factor of deflection (η) and influence factor of bending moment (μ), which are respectively shown in Eq. (4).

$$\eta = \frac{\sin\xi + \cos\xi}{e^{\xi}} \quad , \quad \mu = \frac{-\sin\xi + \cos\xi}{e^{\xi}} \tag{4}$$

where $\xi = x/L$, and "x" is the distance of the calculated point to the loading point and "L" is the characteristic length. The deflection diagram and moment diagram can be obtained by using the following Eqs. (5) and (6), respectively.

$$y = \frac{Q}{2.b.C.L}.\eta \tag{5}$$

$$M = \frac{Q.L}{4}.\mu \tag{6}$$

In his book "Beam on Elastic Foundations", Hetényi developed some equations for various boundary conditions in order to explain the response of the railway track to the vertical wheel forces (Hetényi 1946). The 2D model illustrates for a railway track, a single rail supported by the half width of the track. The vertical depth of the model represents deformation, moments, pressure, or the shear forces developed in the track.

A railway track lays on subgrade and reacts to the vehicle forces together with the subgrade. A "track modulus" term can explain the mutual deformation characteristics of the soil and the railway track, when the railway track is portrayed as a linear structure and its deflection characteristics investigated in two dimensions. Coefficient of vertical subgrade reaction is determined by the plate loading test by using a plate with high bending stiffness subjected to a concentrated loading. When one considers the loaded plate in three dimensions presented in Fig. 2 and represents this plate as a beam supported by an elastic subgrade as in Fig. 5a, one needs to portray the subgrade reaction on a unit length of the beam along x-axis by taking into account the width of the plate along the y-axis. When the same loading conditions are applied to the railway track, the unit force acting on a single rail can be found by multiplying the pressure (p) developed on the subgrade by half of the track width (B). Fig. 5b shows the pressures under a single rail and Eqs. (7) and (8) show the track modulus (u) related to the coefficient of vertical subgrade reaction and the width of the supported plate.

$$u = -\frac{p(x)*B}{y(x)} = -\frac{q(x)}{y(x)} \tag{7}$$

$$u = C \cdot B \tag{8}$$

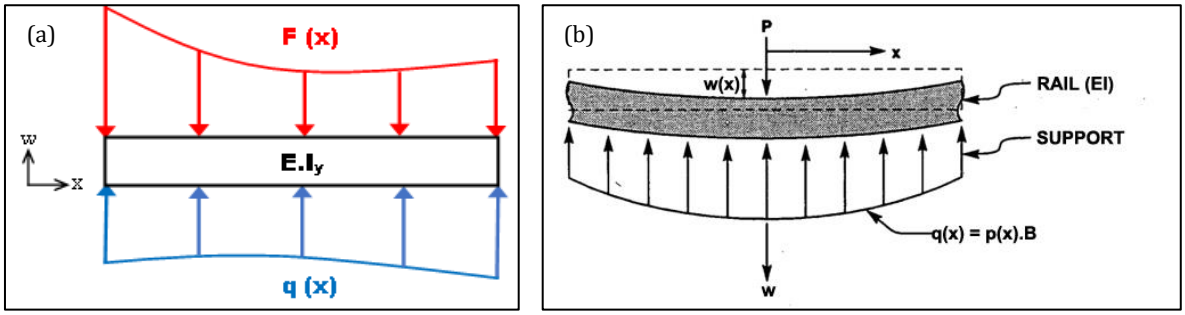

Fig. 5. (a) Two dimensional representation of a plate loaded in three dimensions as a beam; (b) A single rail supported by the half width of the track by Selig and Waters (1994).

The BOEF model offers a "track stiffness" concept which is determined by considering the rigidity of the rail and track modulus. The value of this parameter is highly effective on the general performance of the track (Balcı and Bezgin 2020) and the value of dynamic impact forces developed on the track. Bezgin (2017), Bezgin (2018), Wehbi and Bezgin (2019), and Bezgin and Kolukırık (2020) offers equations that correlates track stiffness and dynamic impact forces on railway tracks. Bezgin (2018) and Bezgin and Wehbi (2019) show that variation of the track stiffness over a specific length of a track leads to the occurrence of additional dynamic impact forces.

When a wheel force of *"P"* is exerted on the track, the maximum deformation w_{max}=$w(0)$ occurs at the point where the wheel contacts the track. Track stiffness (k) is the total track resistance per unit of deformation as shown in Eq. (9) and it is a lumped sum estimate of the total track resistance manifested along the railway track to a unit deformation exerted at a certain location on the rail.

$$k = \frac{P}{w_{\max}} \tag{9}$$

2.3. Discrete elastic support model

Considering that in reality, the rail is not continuously but discretely supported by the sleepers, further models are developed (Fig. 6).

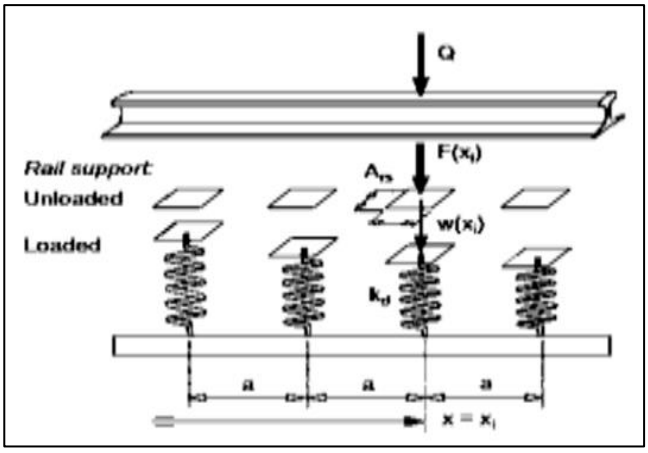

Fig. 6. Discrete support model by Esveld (2001).

When $F(x_i)$ is the vertical force at a i^{th} discrete support (x=x_i), A_{rs} is the effective rail support area, and $w(x_i)$ is the deformation at the point of interest, Winkler's model suggest the correlation shown in Eq. (10).

$$F(x_i) = C.A_{rs}.w(x_i) = k_d.w(x_i) \tag{10}$$

Thus, spring constant of the support is shown in Eq. (11).

$$k_d = C.A_{rs} \tag{11}$$

Spring constant in a homogenously supported track is the ratio of the wheel load to the sum of all measured significant deformations in the vicinity of the load as presented in Eq. (12).

$$k_d = \frac{Q}{\Sigma w} \tag{12}$$

However, spring constant (k_d) is the property of the support and is different than total spring constant of the track i.e. track stiffness (k_{total}). Eq. (13) shows the track stiffness and Eq. (14) correlates track stiffness to the support spring constant.

$$k_{\text{total}} = \frac{Q}{w_{\max}} \tag{13}$$

$$k_d = \frac{w_{\max}}{\Sigma w}.k_{\text{total}} \tag{14}$$

2.4. Talbot's work

One of the most significant contributions to the railway track analysis is made by Arthur Newell Talbot who ran the Engineering Experiment Station at the University of Illinois at Urbana-Champaign. Dr. Talbot has fundamental research, which has been directed since 1914 and summarized under "Stresses in Railroad Track" that forms a basis for railway engineering. Mechanical properties, mode of action, and resistances developed in the various track components under the dynamic forces of locomotives and cars moving at various speeds are investigated by Illinois (2022) to obtain authoritative information. Since the knowledge about the scientific nature of the stresses in railway tracks was very limited at the time the work was begun, the work provided an understanding of the interaction between track and rolling

stock and contributed to a more rational basis for railway track design. Fig. 7 shows the Talbot Committee loading device (1918) setup used to determine rail deflection profiles and the track modulus. There has been no attemp to improve Talbot's procedure until 1960s. Later, efforts have been made by analyzing track as a layered system using finite element analysis (Hay 1991).

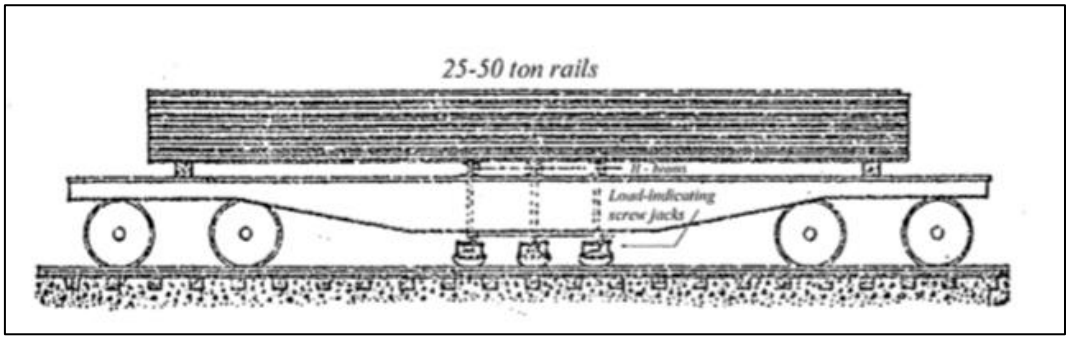

Fig. 7. Talbot Committee loading device (1918) for the analysis of rail deflection profile (Kerr 2003).

3. Analytical Solution of the BOEF Equation

The solution of the 4th-grade differential equation proposed by the BOEF model allows one to obtain the equations of deformation, moment, and shear forces. In this chapter, the solution to this equation will be presented. Eq. (15) correlates track pressure per unit length of track to track stiffness and track deflection.

$$q(x) = -u.y(x) \tag{15}$$

In this equation, u is the track modulus, $y(x)$ is the downward deflection of the foundation under the rail, and $q(x)$ is the downward force from the foundation on the rail per unit length of rail.

Fig. 8 shows a beam on elastic foundation and the forces applied to this beam. This beam is in equilibrium under these forces. The moment equation applied to the beam under the effect of bending is combined with the equilibrium equation. As a result, a differential equation is obtained.

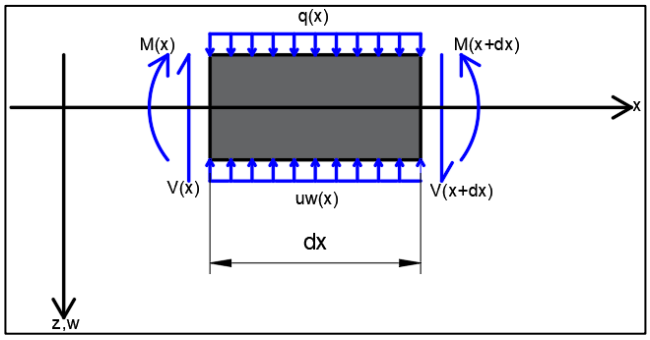

Fig. 8. The forces applied to the beam on elastic foundation.

Eq. (16) presents the equilibrium equation of the beam in Fig. 8 and solves for the variation of the shear force through Eqs. (17) and (18):

$$V - (V + dV) + u.y.dx - qdx = 0 \tag{16}$$

$$-dV + u.y.dx - qdx = 0 \tag{17}$$

$$\frac{dV}{dx} = u.y(x) - q(x) \tag{18}$$

where $V(x)$ is the shear force.

The shear force is obtained by taking the derivative of the moment. In order to write the above equation in terms of moment, the second degree derivative of the moment is taken in Eq. (19).

$$V(x) = \frac{dM(x)}{dx} \rightarrow \frac{dV(x)}{dx} = \frac{d^2M(x)}{dx^2} = u.y(x) - q \tag{19}$$

The moment equation of a beam under bending is shown below. In order to combine this equation with the above equation, the second derivative of the moment equation of the beam under bending is taken as shown in Eq. (20). As a result, a fourth degree derivative is obtained as in Eq. (21). Where E is modulus of elasticity and I is moment of inertia.

$$V(x) = \frac{dM(x)}{dx} \rightarrow \frac{dV(x)}{dx} = \frac{d^2M(x)}{dx^2} = u.y(x) - q \tag{20}$$

$$EI\frac{d^4y}{dx^4} = q(x) - u.y(x) \tag{21}$$

These equations can now be applied to railway tracks. Instead of a distributed vertical load, concentrated point loads (P) will be considered and load distribution will be disregarded such that $q(x)$ = 0. Hence, the general form of Eq. (21) is revised in Eq. (22) and it's special form for $q(x)$=0 is presented in Eq. (23).

$$\frac{d^4y(x)}{dx^4} + \frac{u.y(x)}{EI} = \frac{q(x)}{EI} \tag{22}$$

$$\frac{d^4y(x)}{dx^4} + \frac{u.y(x)}{EI} = 0 \tag{23}$$

After restating the differential equation for beam on elastic foundation, $y(x)$=e^{ax} is proposed as a solution for

$y(x)$. Taking the necessary derivatives of $y(x)$, Eqs. (24-28) are obtained.

$$y(x) = e^{ax} \tag{24}$$

$$y'(x) = a \times e^{ax} \tag{25}$$

$$y''(x) = a^2 \times e^{ax} \tag{26}$$

$$y'''(x) = a^3 \times e^{ax} \tag{27}$$

$$y''''(x) = a^4 \times e^{ax} \tag{28}$$

These equations are inserted into Eq. (23), leading to Eqs. (29-32).

$$y''''(x) + \frac{u.y(x)}{EI} = 0 \tag{29}$$

$$a^4 e^{ax} + \frac{u.e^{ax}}{EI} = 0 \tag{30}$$

$$a^4 e^{ax} = -\frac{u.e^{ax}}{EI} \tag{31}$$

$$a^4 = -\frac{u}{EI} = \frac{u}{EI} \times (-1) = \sqrt[4]{\frac{u}{EI}} \times \sqrt[4]{-1} \tag{32}$$

In the above equation, "a" is of fourth order and has 4 roots. To find these roots, complex numbers and polar representations of complex numbers are used. Eq. (33) presents the complex number representation of -1 and its polar representation in this complex number.

$$-1 = -1 + 0i = r(\cos\theta + i\sin\theta) \tag{33}$$

In polar representation of complex numbers, the distance of the complex number in the coordinate system from the origin is defined by "r".

De Moivre's Theorem (N^{th} Root Theorem) is used to find these roots. Eqs. (34-36) can be used to find the roots of an equation whose polar representation is known by applying De Movrie's Theorem.

$$a_{k'} = \sqrt[n]{r}(\cos(a) + i\sin(\alpha)) \tag{34}$$

$$\alpha = \frac{\theta + 2\pi k}{n} \tag{35}$$

The equation obtained using the above two formulas is shown below.

$$a_{k'} = \sqrt[n]{r}\left(\cos\left(\frac{\theta}{n} + \frac{2\pi k}{n}\right) + i\sin\left(\frac{\theta}{n} + \frac{2\pi k}{n}\right)\right) \tag{36}$$

Substitute of the n and r values in the equations above leads to Eqs. (37-41). The k value starts from 0 and goes up to the n-1 value where n = 4 and r = 1.

$$a_{k'} = \cos\left(\frac{\pi}{4} + \frac{2k\pi}{4}\right) + i\sin\left(\frac{\pi}{4} + \frac{2k\pi}{4}\right) \quad k = 0, 1, 2, 3 \tag{37}$$

$$a_{0'} = \cos\frac{\pi}{4} + i\sin\frac{\pi}{4} = \frac{\sqrt{2}}{2} + i\frac{\sqrt{2}}{2} \tag{38}$$

$$a_{1'} = \cos\left(\frac{\pi}{4} + \frac{2\pi}{4}\right) + i\sin\left(\frac{\pi}{4} + \frac{2\pi}{4}\right) = \cos\frac{3\pi}{4} + i\sin\frac{3\pi}{4} = -\frac{\sqrt{2}}{2} + i\frac{\sqrt{2}}{2} \tag{39}$$

$$a_{2'} = \cos\frac{5\pi}{4} + i\sin\frac{5\pi}{4} = -\frac{\sqrt{2}}{2} - i\frac{\sqrt{2}}{2} \tag{40}$$

$$a_{3'} = \cos\frac{7\pi}{4} + i\sin\frac{7\pi}{4} = \frac{\sqrt{2}}{2} - i\frac{\sqrt{2}}{2} \tag{41}$$

By simplifying the equations above, the following roots shown in Eqs. (42-45) are obtained.

$$a_{0'} = \frac{\sqrt{2}}{2} + i\frac{\sqrt{2}}{2} = \frac{2}{2\sqrt{2}} + \frac{2i}{2\sqrt{2}} = \frac{1+i}{\sqrt{2}} \tag{42}$$

$$a_{1'} = -\frac{\sqrt{2}}{2} + i\frac{\sqrt{2}}{2} = \frac{-1+i}{\sqrt{2}} \tag{43}$$

$$a_{2'} = -\frac{\sqrt{2}}{2} - i\frac{\sqrt{2}}{2} = \frac{-1-i}{\sqrt{2}} \tag{44}$$

$$a_{3'} = \frac{\sqrt{2}}{2} - i\frac{\sqrt{2}}{2} = \frac{1-i}{\sqrt{2}} \tag{45}$$

If these roots are substituted in Eq. (32) and rearrangement of the roots of this equation leads to the values shown in Eqs. (46-49) by considering Eq. (46).

$$a_0 = \sqrt[4]{\frac{u}{EI}} \times \frac{1}{\sqrt{2}}(1+i) = \sqrt[4]{\frac{u}{4EI}} \times (1+i) \tag{46}$$

$$a_1 = \sqrt[4]{\frac{u}{4EI}}(-1+i) \tag{47}$$

$$a_2 = \sqrt[4]{\frac{u}{4EI}}(-1-i) \tag{48}$$

$$a_3 = \sqrt[4]{\frac{u}{4EI}}(1-i) \tag{49}$$

All the equations above have $\sqrt[4]{\frac{u}{4EI}}$ as a common combined parameter. It is represented by β as shown in Eq. (50) for simplification.

$$\beta = \sqrt[4]{\frac{u}{4EI}} \tag{50}$$

Hence, Eqs. (51-54) present a_0, a_1, a_2 and a_3 in terms of β.

$$a_0 = \beta + \beta i \tag{51}$$

$$a_1 = -\beta + \beta i \tag{52}$$

$$a_2 = -\beta - \beta i \tag{53}$$

$$a_3 = \beta - \beta i \tag{54}$$

By writing the roots of "a" in terms of β in the $y(x) = e^{ax}$ equation, Eqs. (55-58) are acquired.

$$\text{for } a_0;\ \ y(x) = e^{a_0 x} = e^{\beta x + i\beta x} \tag{55}$$

$$\text{for } a_1;\ \ y(x) = e^{a_1 x} = e^{-\beta x + i\beta x} \tag{56}$$

$$\text{for } a_2;\ \ y(x) = e^{a_2 x} = e^{-\beta x - i\beta x} \tag{57}$$

$$\text{for } a_3;\ \ y(x) = e^{a_3 x} = e^{\beta x - i\beta x} \tag{58}$$

The solution that includes all solutions of a differential equation is called general solution. There are 4 integral constants for the general solution of the above equation. These constants are called A_1, A_2, A_3 and A_4. The general solution of this differential equation is shown in Eqs. (59-60).

$$y(x) = A_1.e^{a_0 x} + A_2.e^{a_1 x} + A_3.e^{a_2 x} + A_4.e^{a_3 x} \tag{59}$$

$$y(x) = A_1.e^{\beta x + i\beta x} + A_2.e^{-\beta x + i\beta x} + A_3.e^{-\beta x - i\beta x} + A_4.e^{\beta x - i\beta x} \tag{60}$$

Euler has a solution for the $e^{i\beta x}$ expansion called the Euler Formula shown in Eq. (61).

$$e^{i\beta x} = \cos(\beta x) + i\sin(\beta x) \tag{61}$$

Substituting Euler's formula in the general solution of the differential equation, Eq. (62) is obtained.

$$y = A_1.e^{\beta x}(\cos\beta x + i\sin\beta x) + A_2.e^{-\beta x}(\cos\beta x + i\sin\beta x) + A_3.e^{-\beta x}(\cos\beta x - i\sin\beta x) + A_4.e^{\beta x}(\cos\beta x - i\sin\beta x) \tag{62}$$

The above equation is simplified in Eq. (63). The new constant values in the equation are then denoted by C_n as shown in Eqs. (64-67).

$$y = e^{\beta x}[(A_1 + A_4)\cos(\beta x) + (A_1 i - A_4 i)\sin(\beta x)] + e^{-\beta x}[(A_2 + A_3)\cos(\beta x) + (A_2 i - A_3 i)\sin(\beta x)] \tag{63}$$

$$(A_1 + A_4) = C_1 \tag{64}$$

$$(A_1 i - A_4 i) = C_2 \tag{65}$$

$$(A_2 + A_3) = C_3 \tag{66}$$

$$(A_2 i - A_3 i) = C_4 \tag{67}$$

Eq. (68) presents the general solution for displacement is as follows.

$$y(x) = e^{\beta x}[C_1.\cos(\beta x) + C_2.\sin(\beta x)] + e^{-\beta x}[C_3.\cos(\beta x) + C_4.\sin(\beta x)] \tag{68}$$

Following the attainment of this general solution is obtained, one can apply its particular solution to railway engineering. One can consider infinite beam or rail loaded with a singular P force at $x = 0$. C_1 and C_2 terms lead to infinite deflection (y) when $x \to \infty$ at the right of the beam. This is contrary to the boundary conditions of the beam. When $C_1 = C_2 = 0$, only half of the equation remains and the deflection is zero when $x \to \infty$, which is in agreement with the boundary conditions. Such being the case, Eq. (69) represents the special form of Eq. (68) when applied to an continous railway track supported by subgrade. The derivatives of this written equation are shown in Eqs. (70-72).

$$y(x) = e^{-\beta x}[C_3\cos(\beta x) + C_4\sin(\beta x)] \tag{69}$$

$$y'(x) = \beta e^{-\beta x}[(-C_3 + C_4)\cos(\beta x) + (-C_3 - C_4)\sin(\beta x)] \tag{70}$$

$$y''(x) = \beta^2 e^{-\beta x}[-2C_4\cos(\beta x) + 2C_3\sin(\beta x)] \tag{71}$$

$$y'''(x) = \beta^3 e^{-\beta x}[2(C_3 + C_4)\cos(\beta x) + (-C_3 + C_4)\sin(\beta x)] \tag{72}$$

The singular force P acting on the rails is applied from the x=0 point. Eq. (68) applies for the whole track except the point that load is applied. The deflection and bending moment at the load P is not known. However, the shear force at that point is known and can be obtained by taking the derivative of the moment variation along the supported track. Since the point load P is symmetrically supported by a homogenenous track, the maximum value of the shear forces to the immediate right and left of the location where the load P is acting is $P/2$. Hence, Eq. (73) presents the shear force $V(x)$ and it has maximum value at x=0.

$$V(x) = \frac{dM(x)}{dx} = EI.y'''(x) \to for\ x = 0, V_{\max} = \frac{P}{2} \tag{73}$$

Substituting the third derivative of the displacement in this equation, Eq. (74) is obtained.

$$V(x) = EI(\beta^3 e^{-\beta x}[2(C_3 + C_4)\cos(\beta x) + 2(-C_3 + C_4)\sin(\beta x)]) \tag{74}$$

Eq. (75) results for $x = 0$, where $C_3 + C_4$ is presented in Eq. (76).

$$2EI\beta^3(C_3 + C_4) = \frac{P}{2} \tag{75}$$

$$C_3 + C_4 = \frac{P}{4EI\beta^3} \tag{76}$$

The derivative of the beam's displacement function gives the slope. Since it is a symmetrical system, the slope at $x = 0$ is equal to 0. In this case, $y' = 0$ shown in Eq. (77) and solved through Eqs. (78-79).

$$y'(x) = \beta e^{-\beta x}[(-C_3 + C_4)\cos(\beta x) + (-C_3 - C_4)\sin(\beta x)] = 0 \quad (77)$$

$$\beta e^{0}[(-C_3 + C_4)\cos(0) + (-C_3 - C_4)\sin(0)] = 0 \quad (78)$$

$$\beta(-C_3 + C_4) = 0 \quad (79)$$

β is a fourth-degree root. So this cannot be equal to 0 and hence the part in parentheses must be equal to 0 as shown in Eq. (80).

$$C_4 - C_3 = 0 \rightarrow C_3 = C_4 = C \quad (80)$$

If the above equations are combined, Eq. (81) is obtained where *"u"* is presented in Eq. (82) and C_3 and C_4 are presented in Eq. (83).

$$2C = \frac{P}{4EI\beta^3} \rightarrow C = \frac{P}{8EI\beta^3} \quad (81)$$

$$u = 4EI\beta^4 \quad (82)$$

$$C_3 = C_4 = C = \frac{P\beta}{2u} \quad (83)$$

As a result of the calculations, the displacement formula on the railway lines has been simplified in Eqs. (84) and (85).

$$y(x) = e^{-\beta x}[C_3\cos(\beta x) + C_4\sin(\beta x)] \quad (84)$$

Since $C_3 = C_4$;

$$y(x) = e^{-\beta x}[C_3\cos(\beta x) + C_3\sin(\beta x)] \quad (85)$$

By placing the equation in C_3 brackets into the equation above, one obtains the Eqs. (86) and (87).

$$y(x) = C_3 e^{-\beta x}[\cos(\beta x) + \sin(\beta x)] \quad (86)$$

Eq. (87) is the general formula of the displacement under the rail on the railway lines.

$$y(x) = \frac{P\beta}{2u} e^{-\beta x}[\cos(\beta x) + \sin(\beta x)] \quad (87)$$

1st, 2nd and 3rd order derivatives of the above displacement equation when multiplied by *EI*, gives the slope, moment and shear distribution along the track.

Taking the 1st derivative of the displacement function through Eqs. (88) and (89) results in Eq. (90) for the general equation for the variation of the slope along the deflected track:

$$y'(x) = -\frac{P\beta^2}{2u}(\cos(x\beta) + \sin(\beta x)) + \frac{P\beta^2}{2k} e^{-\beta x}(-\beta\sin(\beta x) + \cos(\beta x)\,\beta) \quad (88)$$

$$\frac{P\beta^2}{2u} e^{-\beta x}(-\cos(\beta x) - \sin(\beta x) - \sin(\beta x) + \cos(\beta x)) \quad (89)$$

$$y'(x) = \frac{P\beta^2}{2u} e^{-\beta x}(-2\,sin(\beta x)) \quad (90)$$

Second derivative of the deflection equation results in the general equation of moment along the track:

$$y''(x) = -\frac{P\beta^3}{2u} e^{-\beta x}(-2\sin(\beta x)) + \frac{P\beta^3}{2u} e^{-\beta x}(-2\cos(\beta x)) \quad (91)$$

$$y''(x) = \frac{P\beta^3}{2u} e^{-\beta x}(2\sin(\beta x) - 2\cos(\beta x)) = \frac{P\beta^3}{u} e^{-\beta x}(\sin(\beta x) - \cos(\beta x)) \quad (92)$$

$$M(x) = -EIy''(x) \rightarrow EI = \frac{u}{4\beta^4} \rightarrow -\frac{u}{4\beta^4}\frac{P\beta^3}{u} e^{-\beta x}(\sin(\beta x) - \cos(\beta x)) \quad (93)$$

$$M(x) = \frac{P}{4\beta} e^{-\beta x}(\cos(\beta x) - \sin(\beta x)) \quad (94)$$

The 3rd derivative of the deflection equation results in the general equation of shear force along the track:

$$y'''(x) = -\frac{P\beta^4}{u} e^{-\beta x}(\sin(\beta x) - \cos(\beta x)) + \frac{P\beta^4}{u} e^{-\beta x}(\cos(\beta x) + \sin(\beta x)) \quad (95)$$

$$y'''(x) = \frac{P\beta^4}{u} e^{-\beta x}(-\sin(\beta x) + \cos(\beta x) + \cos(\beta x) + \sin(\beta x)) = \frac{P\beta^4}{u} e^{-\beta x} \times 2 \times \cos(\beta x) \quad (96)$$

$$V(x) = \frac{dM(x)}{dx} = -EI.w'''(x) = -\frac{u}{4\beta^4}\frac{P\beta^4}{u} e^{-\beta x} \times 2 \times \cos(\beta x) \quad (97)$$

$$V(x) = \frac{P}{2} e^{-\beta x}\cos(\beta x) \quad (98)$$

The pressure is obtained in Eq. (101) by multiplying the track deflections by k as shown in Eqs. (99) and (100).

$$P(x) = u.w(x) \quad (99)$$

$$w(x) = y = \frac{P\beta}{2u} e^{-\beta x}(\cos(\beta x) + \sin(\beta x)) \quad (100)$$

$$P(x) = u.w(x) = u\frac{P\beta}{2u} e^{-\beta x}(\cos(\beta x) + \sin(\beta x) = \frac{P\beta}{2} e^{-\beta x}(\cos(\beta x) + \sin(\beta x) \quad (101)$$

Maximum bending moment, maximum shear stress, and maximum intensity of pressure against the rail are shown in Eqs. (102-104).

$$M_{\max} = P(\frac{EI}{64u})^{1/4} \quad (102)$$

$$V_{\max} = -P/2 \tag{103}$$

$$P_{\max} = P\left(\frac{u}{64EI}\right)^{1/4} \tag{104}$$

The "u" term used in the equations is used to describe "track modulus". Eq. (105) shows the relation between track stiffness (k) and track modulus (u).

$$k = \frac{2u}{\beta} = \sqrt[4]{64.E.I.u^3} \tag{105}$$

Track stiffness values can vary highly from site to site. In Li and Berggren's work (2010), 32 kN/mm track stiffness is evaluated as "soft track", whereas 78 kN/mm is described as "normal track" and 172 kN/mm is "stiff track".

Minimization of the energy released by materials during the deformation (called elastic strain energy) can be used to find optimum track stiffness. Wehbi and Musgrave (2017) carried out the experiments for British Railways and concluded that a minimum of elastic strain energy can be reached while track stiffness goes to 160 kN/mm. However, it is seen that the effect of the strain energy is reduced after the track stiffness of 45 kN/mm. Therefore, the optimum value can be chosen as 45 kN/mm. Lopez Pite et al. (2004), on the other hand, suggests optimum track stiffness of 70-80 kN/mm by optimizing maintenance costs and dissipated energy. However, higher track stiffness values can be seen depending on the support conditions. For instance, the stiffness of the ballasted track laying on the bridge is found to be 109 kN/mm and the ballastless track in the tunnel is found to be 203 kN/mm in the measurements taken by Zhao et al (2015) from a part of the Shanghai-Kunming railway line.

While the track modulus of a soft track can be low as 7 MPa, stiff tracks can be high as 80 MPa. When the optimum track stiffness values stated in the literature is considered, the optimum values of track modulus should be between 20 to 45 MPa when UIC 60 rail type is used.

4. Shortcomings of the BOEF Model

While the BOEF model offers a practical and simple solution for the analysis of the railway tracks, there are some points where it deviates from the real track conditions because of the assumptions it make. Since the BOEF model is developed based on the Winkler model, those shortcomings are valid for BOEF as well.

According to the deformation values calculated using the BOEF model, the maximum deformation value occurs under the point where the wheel contacts the track. As one moves away from this point, the deformation gradually decreases. If the wheel is at a certain distance from the point of contact with the track, there is a reverse deformation due to the tensile forces on the track. Track deformations for different track bed moduli are shown in Fig. 9(a) and moments are shown in Fig. 9(b). As the track stiffness decreases, the maximum deformation in the track increases together with the value of reverse deformation. The reverse deformation means the compressive stress must be negative at the points of interest. In reality, however, such a tensile force does not occur in the subgrade. In fact, the formation of negative stress is not physically possible because the ballast layer cannot absorb the tensile force (Esveld 2001). Hence, the maximum deformation value offered by the BOEF equations under the single wheel force is different than the actual deformation value. This should be taken into account during design. In order to overcome this problem, deformation calculations can be balanced by using some optimization programs.

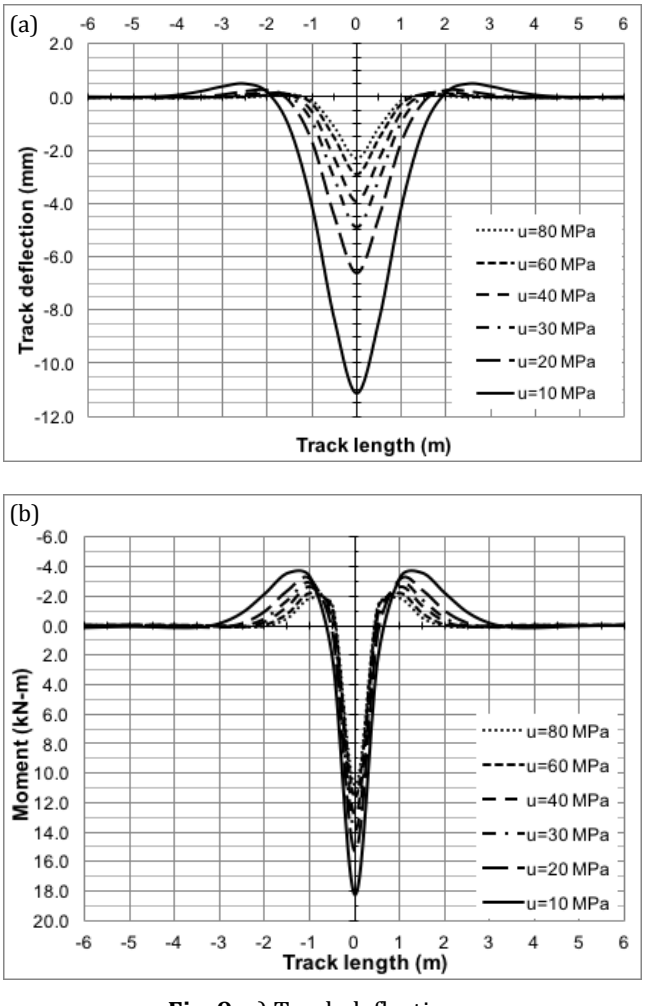

Fig. 9. a) Track deflections;
b) Moments for various track bed moduli values.

This situation is similar to a simple beam calculation shown in Fig. 10. While negative moments occur at the endpoints of a beam with fixed supports, a maximum positive moment occurs in the span. Being constrained at the endpoints ensures that the beam is supported at the ends and this reduces the moment in the mid-span. However, one can assume as the supports at the ends of this beam can be loosened, its bending stiffness can be reduced, and the same beam may become a simply supported beam. In this case, since the beam cannot receive a response from the endpoints, a negative moment does not occur here. The negative moments occurring at the

endpoints in the first case are now collected in the middle span and the maximum positive moment in the middle span increases. In Fig. 10, the moments occurring in a fixed beam and a simply supported beam are presented. Likewise, in the railway track example, the assumed negative moments to occur at the ends of the deformation curve or a certain percentage of it be added to the point where the wheel contacts the track, i.e. the point where the maximum positive moment occurs. According to one source, the regions where rail is raised above ground level must be pulled down by the ground at 4% of the maximum pressure under load (Hartog 1987). Since the ground cannot actually pull onto a track, a part of the positive moment shown in Fig. 10 will likely collect along the negative moment region. Kerr, in his book highlights his particular research on the topic and concentrates on the variations of the moments and deflections along the uplifted track region (Kerr 2003) and suggests the amount of variations along the actual track with regards to the estimated behavior by the BOEF theorem.

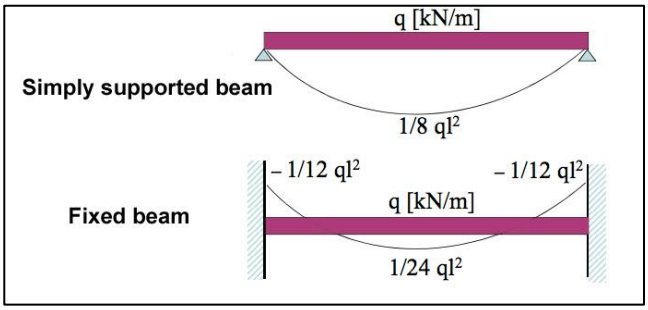

Fig. 10. Moments in the fixed and simply supported beam.

On the other hand, although the BOEF model assumes that the track is constantly supported, this support is impaired at specific points where there are geometric profile changes, such as insulated rail joints and turnouts. In such cases, the modified BOEF should be used in calculations. Kerr (2003) offered some equations for the two-axle trucks near a poorly maintained joint. Poorly maintained joint means an area where bending moments are not transferred to the adjacent rail and thus, neighboring rails act independently as shown in Fig. 11. Eq. (106) shows the deformation and Eq. (107) shows the bending moments in this case.

$$w(x) = \frac{P\beta}{2k}\{4e^{-\beta x}\cos\beta x + e^{-\beta|x-b|}[\cos\beta|x-b| + \sin\beta|x-b|] + +e^{-\beta|x+b|}[\cos\beta|x+b| + \sin\beta|x+b|] + 2e^{-\beta|x+b|}[\cos\beta(x-b) - \sin\beta(x-b)]\} \quad (x>0) \quad (106)$$

$$M(x) = -EIw''(x) = -\frac{P}{4\beta}\{4e^{-\beta x}\sin\beta x + e^{-\beta|x-b|}[\sin\beta|x-b| - \cos\beta|x-b|] + e^{-\beta|x+b|}[\sin\beta|x+b| - cos\beta|x+b|] + 2e^{-\beta|x+b|}(\cos\beta b - \sin\beta b)(\cos\beta x + \sin\beta x)\} \quad (107)$$

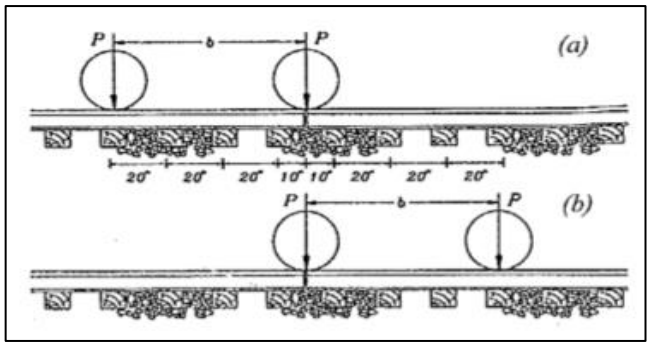

Fig. 11. 2-axle truck positions near a poorly maintained joint represented by Kerr (2003).

5. Comparison of Continuous Rail and Rail End Cases

All calculations within this chapter are done for UIC 60 rail type. Figs. 12 and 13 compare the deformations and moments of a continuous rail and a rail-end case under a 2-axle bogie with an axle spacing of 2 m, UIC 60 rail profile, and k=120 kN/mm track stiffness. One can see that maximum track deformation is the highest when the wheel contacts the rail-end point. The deformation under the second wheel is also relatively higher compared to the deformation of the continuous rail. The maximum negative bending moment occurs between the neighboring wheels and is higher for the rail-end case. However, the moment equals to zero at the point where rail is ended. The first cross-tie near a rail joint is subjected to the rail seat force that is at least three times larger than the force applied to the normal ties without joint or far away from the joint (Kerr 2003).

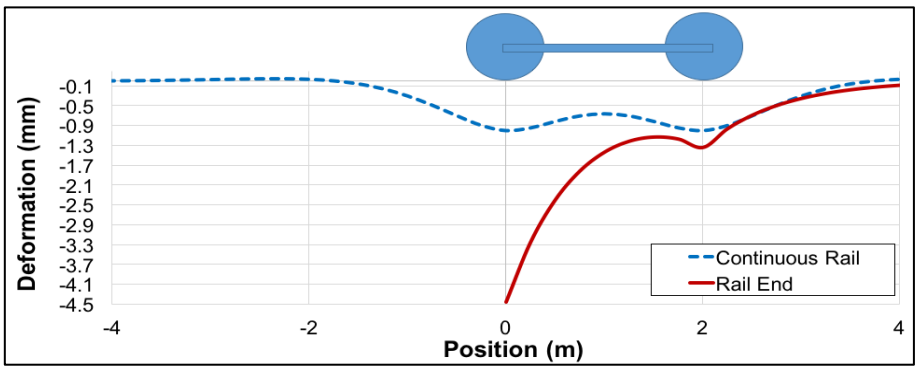

Fig. 12. Comparison of the deformations for continuous rail and rail-end.

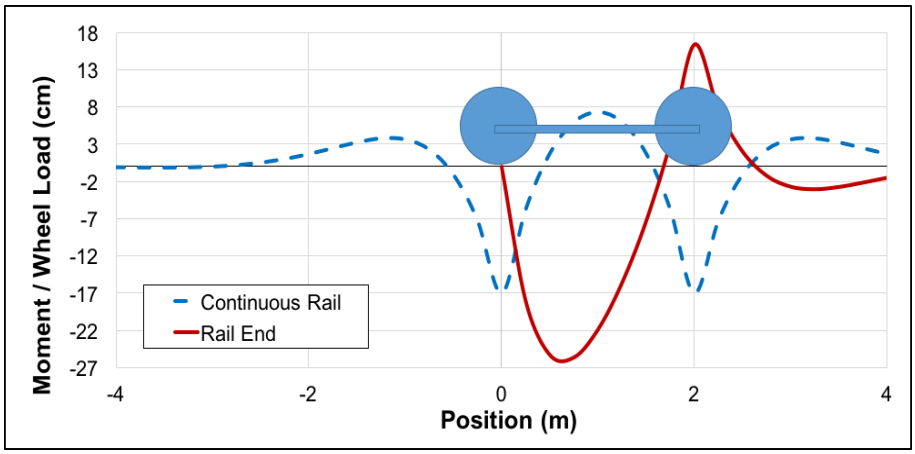

Fig. 13. Comparison of the moments for continuous rail and rail-end.

Figs. 14(a) and 14(b) show the deformations of continuous rail and the rail-end case for track stiffness varying between k=20 kN/mm and k=120 kN/mm. While track stiffness changes from k=20 kN/mm to k=120 kN/mm, the ratio of the maximum deformation of the continuous rail to the rail-end case varies between 3.6 and 4.4, respectively. In other words, the stiffness of the discontinuous track is about 25% of the stiffness of the continuous track on average.

Figs. 15(a) and 15(b) represent the ratio of the moments to the wheel loads for continuous rail and rail-end cases for different track stiffness values. While track stiffness varies between k=20 kN/mm and k=120 kN/mm, the ratio of the maximum negative moment of the continuous rail to the rail-end case is approximately 1.5 for all track stiffness values. These findings show that rail requires more bending capacity in rail joint case and also dynamic impact factor can be higher due to this abrupt variations in track stiffness, which causes the track to deteriorate more throughout its service life.

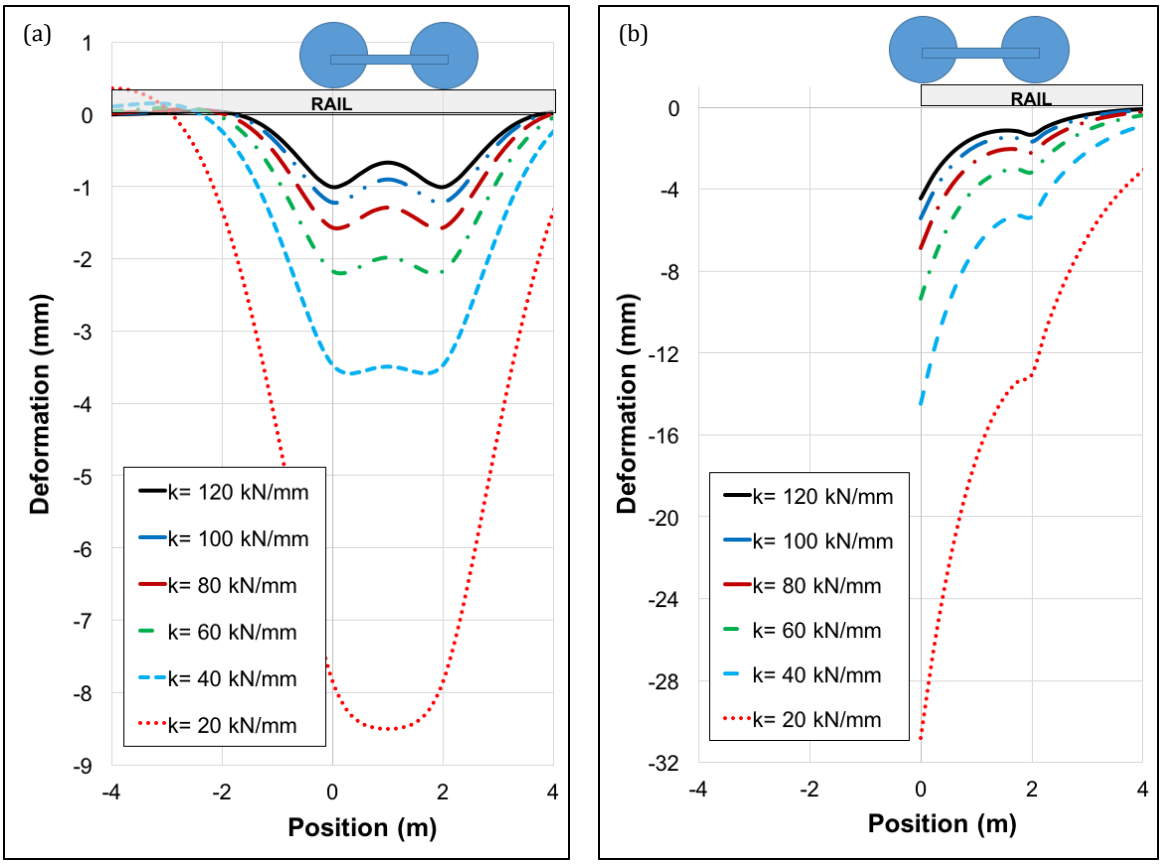

Fig. 14. Deformations at a) continuous rail and b) rail-end for various track stiffness values.

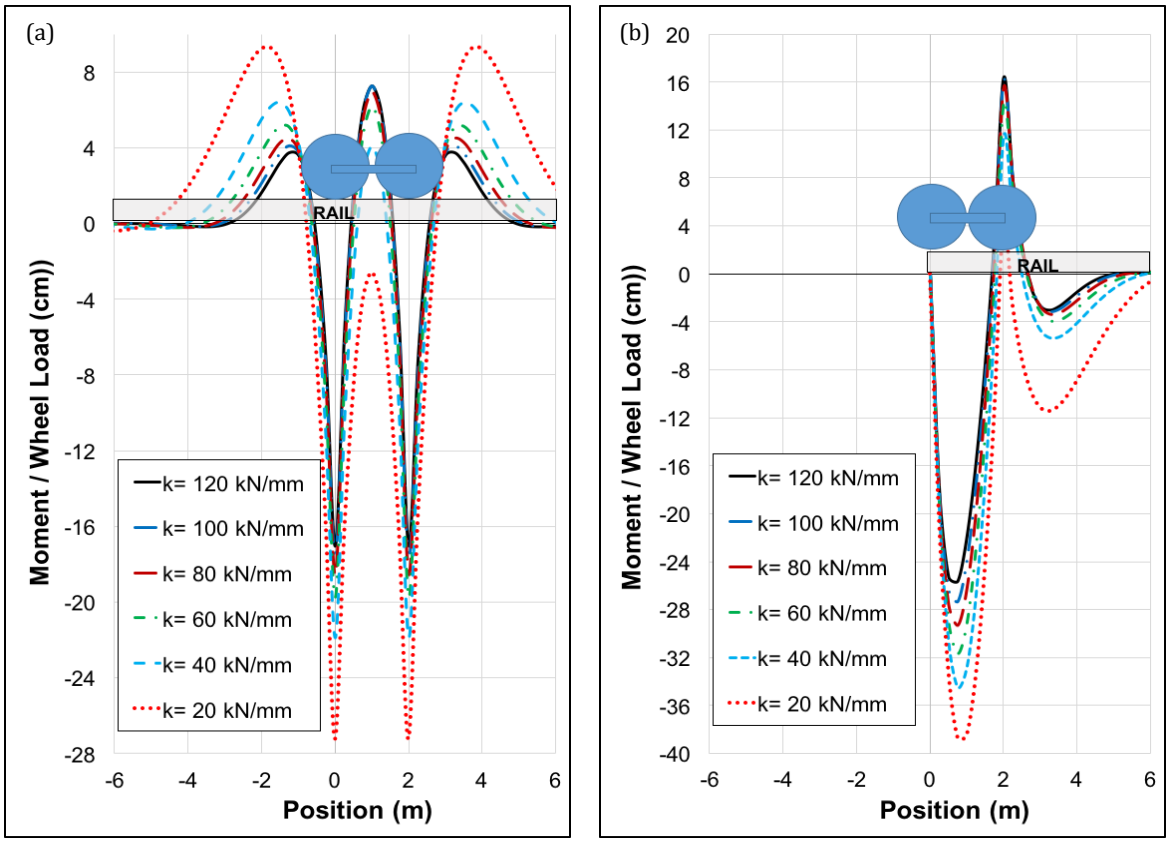

Fig. 15. Moments at a) continuous rail and b) rail-end for various track stiffness values.

6. Conclusions

Development of a mathematical analysis for design of railway tracks became necessary for better understanding and assessment of their responses towards the end of 19th Century. Since railway tracks are directly supported by the subgrade and they are a union of different structural elements, both the analysis of the interaction of the subgrade with the structure and the mutual interaction of the railway components should be well understood for the analysis of the railway tracks. There is also an interaction between the track superstructure and the train as it is directly exposed to train wheel forces. This study, presented an insight into the historic development of the BOEF approach in railway track analyses and provides a mathematical perspective into the development of the response parameters of the railway track.

Although analyzes using the finite element method are quite common today, these analyzes require plenty of time, computational power and also detailed material and geometrical knowledge about the properties of the track's components. For this reason; deformation, moment and shear force calculations can be still made using the BOEF model. These analysis equations are obtained as a result of solving the 4th order differential equation presented by the BOEF model. The step-by-step solution of this differential equation is presented in this study. Afterwards, the difference between the BOEF model and the real railway track case due to the assumptions made are discussed. The BOEF theory, with its explicit nature, continues to support engineers and researchers in their assessment and understanding of railway track mechanics.

Acknowledgements

None declared.

Funding

The authors received no financial support for the research, authorship, and/or publication of this manuscript.

Conflict of Interest

The authors declared no potential conflicts of interest with respect to the research, authorship, and/or publication of this manuscript.

References

Abouelregal AE (2021). Thermoelastic fractional derivative model for exciting viscoelastic microbeam resting on Winkler foundation. *Journal of Vibration and Control*, 27(17-18), 2123-2135.

Aizikovich SM, Mitrin BI, Seleznev NM, Wang YC, Volkov SS (2016). Influence of a soft FGM interlayer on contact stresses under a beam on an elastic foundation. *Structural Engineering and Mechanics: An International Journal*, 58(4), 613-625.

Arnold K (2003). Fundamentals of Railway Track Engineering. Simmons-Boardman Books, Inc., Nebraska.

Balabušić M, Folić B, Ćorić S (2019). Bending the foundation beam on elastic base by two reaction coefficient of Winkler's subgrade. *Open Journal of Civil Engineering*, 9, 123-134.

Balcı E, Bezgin NÖ, Wehbi M (2022). Variation of track response to wheel forces with bogie axle spacing: Apparent track stiffness and its influence on dynamic impact forces on railway tracks. *Transportation Research Record*, 2676(4), 570-588.

Balcı E, Bezgin N (2020). Hat esneme direncinin hat performansı üzerindeki etkileri. *Demiryolu Mühendisliği*, 11, 75-85. (in Turkish)

Balcı E, Yalçın E, Yelce TU, Bezgin NÖ (2021). Bir demiryolu hattının birim esneme direnci üzerinde etkisi olan mekanik ve geometrik niteliklerin incelenmesi. *Mühendislik Bilimleri ve Tasarım Dergisi*, 9(4), 1408-1423. (in Turkish)

Bezgin NÖ (2017). Development of a new and an explicit analytical equation that estimates the vertical dynamic impact loads of a moving train. *Procedia Engineering*, 189C, 2-10.

Bezgin NÖ (2018). An insight into design of prefabricated and prestressed concrete monoblock railway ties for service loads. *Challenge Journal of Structural Mechanics*, 4(4), 126-136.

Bezgin NÖ (2018). Application of a new concept and a method to estimate the vertical impact forces on railway tracks because of track profile irregularities. *97th Annual Meeting of the Transportation Research Board,* Washington, D.C.

Bezgin NÖ (2018). Proposal of a new analytical method to estimate the vertical impact forces on railway tracks because of changes in track profile and track stiffness. *Proceedings of the 5th International Conference on Road and Rail Infrastructure CETRA*, Zadar, Croatia, 837–845.

Bezgin NÖ, Kolukırık C (2020). Applications and estimate comparisons of bezgin–kolukırık equations for dynamic impact forces because of wheel flats with numerical analysis estimates and instrumented track measurements. *Transportation Research Record: Journal of the Transportation Research Board*, 2674(10), 199- 214.

Bezgin NÖ, Wehbi M (2019). Advancement and application of the bezgin method to estimate the effects of stiffness variations along railways on wheel forces. *Transportation Research Record: Journal of the Transportation Research Board*, 2673(7), 248-264.

Campione G, Cannella F, Zizzo M (2021). Flexural response of reinforced concrete beam on elastic foundation under vertical load and bending moment: review of existing methods and proposed new method. *Practice Periodical on Structural Design and Construction*, 26(2), 04021007.

Chandler TG, Vella D (2020). Validity of Winkler's mattress model for thin elastomeric layers: beyond Poisson's ratio. *Proceedings of the Royal Society A*, 476(2242), 20200551.

Datta SC, Roy R (2002). A critical review on idealization and modeling for interaction among soil – foundation - structure system. *Computers and structures*, 80(2-21), 1579-1594.

Esveld C (2001). Modern Railway Track (vol. 385). Zaltbommel: MRT-productions.

Froio D, Verzeroli L, Ferrari R, Rizzi E (2021). On the numerical modelization of moving load beam problems by a dedicated parallel computing FEM implementation. *Archives of Computational Methods in Engineering*, 28(4), 2253-2314.

Hartog DPJ (1987) Advanced Strength of Materials. Dover Publications Inc., New York.

Hay WW (1991). Railroad Engineering (vol. 1). John Wiley & Sons.

Hetenyi M (1946). Beams on Elastic Foundation: Theory with Applications in the Fields of Civil and Mechanical Engineering (vol. 16). University of Michigan Press, Ann Arbor, MI.

Horvath JS (1983a). Modulus of subgrade reaction: new perspective. *Journal of Geotechnical Engineering*, 109(12), 1591–1596.

Horvath JS (1983b). New subgrade model applied to mat foundations. *Journal of Geotechnical Engineering,* 109(12), 1567-1587.

Horvath JS (2002). Basic SSI Concepts and Applications Overview. Soil-Structure Interaction Research Project, Report No. CGT-2002-2, Manhattan College, School of Engineering, New York.

Illinois, Railtec University of Illinois at Urbana-Champaign (2022). Arthur Newell Talbot (1857-1942). https://railtec.illinois.edu/arthur-newell-talbot/

Jones R, Xenophontos J (1977). The Vlasov Foundation Model. *International Journal of Mechanical Sciences,* 19, 317-323.

Kerr AD (1964). Elastic and viscoelastic foundation models. *Journal of Applied Mechanics*, *ASME*, 25(80), 491-498.

Kerr AD (1976). On the stress analysis of rails and ties. *Proceedings of the American Railway Engineering Association*, 78.

Kerr AD (2003). Fundamentals of Railway Track Engineering. Simmons–Boardman Publishing Corporation.

Li MXD, Berggren EG (2010). A study of the effect of global track stiffness and its variations on track performance: simulation and measurement. *Proceedings of the Institution of Mechanical Engineers, Part F: Journal of Rail and Rapid Transit*, 224(5), 375-382.

Lopez Pita A, Teixeira PF, Robuste F (2004). High speed and track deterioration: the role of vertical stiffness of the track. *Proceedings of the Institution of Mechanical Engineers, Part F: Journal of Rail and Rapid Transit*, 218(F1), 31-40.

Onu G (2000). Shear effect in beam finite element on two-parameter elastic foundation. *Journal of Structural Engineering,* 126(9).

Pasternak PL (1954). Fundamentals of the new method of calculating foundations on elastic base using two bed coefficients. *Gosstroyizdat*, 56.

Poddubny AA, Gordon VB (2021). Dynamic loading of the rod at a sudden change of elastic foundation structure. *IOP Conference Series: Materials Science and Engineering*. IOP Publishing, 042076.

Prakoso PB (2012). The basic concepts of modelling railway track systems using conventional and finite element methods. *Info-Teknik*, 13(1), 57-65.

Reissner E (1958). A note on deflections of plates on a viscoelastic foundation. *Journal of Applied Mechanics*, *ASME*, 25(80), 144-145.

Sadeghi J (1997). Investigation of Characteristics and Modelling of Railway Track System. *Ph.D. thesis*, University of Wollongong, Australia.

Sadeghi J, Barati P (2010). Evaluation of conventional methods in analysis and design of railway track system. *International Journal of Civil Engineering*, 8(1), 44-56.

Selig ET, Waters JM (1994). Track Geotechnology and Substructure Management. Thomas Telford, London.

Skar A, Klar A, Levenberg E (2019). Load-independent characterization of plate foundation support using high-resolution distributed fiber-optic sensing. *Sensors,* 19(16), 3518.

Steidl M (2007). Standards and tests of fastening systems. *AREMA Annual Conference Presentation.*

Terzaghi K (1955). Evaluation of coefficients of subgrade reaction. *Geotechnique*, 5(4), 297-326.

Tivari K, Kuppa R (2014). Overview of methods of analysis of beams on elastic foundation. *IOSR Journal of Mechanical and Civil Engineering*, 11(5), 22-29.

Vallabhan CVG, Das YC (1988). Parametric study of beams on elastic foundations. *Journal of Engineering Mechanics,* 114(12), 2072-2082.

Vlasov VZ, Leont'ev UNA (1966). Beams plates and shells on elastic foundations. Kudüs, Israel, Israel Programme for Scientific Translations.

Wang YH, Tham LG, Cheung YK (2005). Beams and plates on elastic foundations: a review. *Progress in Structural Engineering and Materials,* 7(4), 174-182.

Wehbi M, Bezgin NÖ (2019). Proposal and application of a new technique to forecast railway track damage due to track profile variations. *Transportation Research Record: Journal of the Transportation Research Board*, 2673(4), 568-582.

Wehbi M, Musgrave P (2017) Optimisation of track stiffness on the UK railways. *Permanent Way Institute Journal*, 135.

Worku A (2009). Winkler's single-parameter subgrade model from the perspective of an improved approach of continuum-based subgrade modeling. *Zede Journal*, 26, 11-22.

Zhao C, Wang P, Yi Q, Meng D (2015). Application of polyurethane polymer and assistant rails to settling the abnormal vehicle-track dynamic effects in transition zone between ballastless and ballasted track. *Shock and Vibration*, 2015, 826362.